Munc18-2, but not Munc18-1 or Munc18-3, controls compound and single-vesicle–regulated exocytosis in mast cells

Received for publication, February 14, 2018, and in revised form, March 20, 2018 Published, Papers in Press, March 29, 2018, DOI 10.1074/jbc.RA118.002455

Berenice A. Gutierrez[‡§1], Miguel A. Chavez[‡¶], Alejandro I. Rodarte[‡¶], Marco A. Ramos[‡], Andrea Dominguez[¶], Youlia Petrova[‡], Alfredo J. Davalos[‡], Renan M. Costa[‖], Ramon Elizondo[¶], Michael J. Tuvim[‡], Burton F. Dickey[‡], Alan R. Burns[**], Ruth Heidelberger[‡‡], and Roberto Adachi[‡2]

From the [‡]Department of Pulmonary Medicine, University of Texas M. D. Anderson Cancer Center, Houston, Texas 77030, the [§]Escuela de Ingeniería y Ciencias, Tecnologico de Monterrey, Monterrey NL 64849 México, the [¶]Escuela de Medicina y Ciencias de la Salud, Tecnologico de Monterrey, Monterrey NL 64710 México, the [‖]Graduate School of Biomedical Sciences and the [‡‡]Department of Neurobiology and Anatomy, McGovern Medical School, University of Texas Health Science Center, Houston, Texas 77030, and the [**]College of Optometry, University of Houston, Houston, Texas 77204

Edited by Peter Cresswell

Mast cells (MCs) play pivotal roles in many inflammatory conditions including infections, anaphylaxis, and asthma. MCs store immunoregulatory compounds in their large cytoplasmic granules and, upon stimulation, secrete them via regulated exocytosis. Exocytosis in many cells requires the participation of Munc18 proteins (also known as syntaxin-binding proteins), and we found that mature MCs express all three mammalian isoforms: Munc18-1, -2, and -3. To study their functions in MC effector responses and test the role of MC degranulation in anaphylaxis, we used conditional knockout (cKO) mice in which each Munc18 protein was deleted exclusively in MCs. Using recordings of plasma membrane capacitance for high-resolution analysis of exocytosis in individual MCs, we observed an almost complete absence of exocytosis in Munc18-2–deficient MCs but intact exocytosis in MCs lacking Munc18-1 or Munc18-3. Stereological analysis of EM images of stimulated MCs revealed that the deletion of Munc18-2 also abolishes the homotypic membrane fusion required for compound exocytosis. We confirmed the severe defect in regulated exocytosis in the absence of Munc18-2 by measuring the secretion of mediators stored in MC granules. Munc18-2 cKO mice had normal morphology, development, and distribution of their MCs, indicating that Munc18-2 is not essential for the migration, retention, and maturation of MC-committed progenitors. Despite that, we found that Munc18-2 cKO mice were significantly protected from anaphylaxis. In conclusion, MC-regulated exocytosis is required for the anaphylactic response, and Munc18-2 is the sole Munc18 isoform that mediates membrane fusion during MC degranulation.

Mast cells (MCs)[3] derive from hematopoietic progenitors, circulate in immature form, and migrate into different tissues where they complete their differentiation. The widespread distribution of MCs throughout the body favors fast immune and inflammatory responses, including anaphylaxis (1, 2). To accomplish this, MCs release a variety of mediators through several mechanisms, including regulated exocytosis. During exocytosis, the membrane of a secretory vesicle fuses with the plasma membrane, releasing its cargo into the extracellular space and translocating proteins associated with or integral to its membrane to the plasma membrane. Regulated exocytosis in MCs (MC degranulation) is characterized by the almost immediate release of mediators that are premade and stored in large secretory vesicles (MC granules), such as histamine, MC proteases, and other enzymes. This requires MC activation by stimuli that usually employ Ca^{2+} and diacylglycerol as second messengers (3, 4). Degranulation in MCs uses both single-vesicle and compound exocytosis (5, 6). In single-vesicle exocytosis, the membrane of a single MC granule fuses with the plasma membrane. In multivesicular compound exocytosis, granules fuse with each other before fusing with the plasma membrane. In sequential compound exocytosis, granules fuse with granules already fused with the plasma membrane. Both forms of compound exocytosis allow the rapid discharge of granules located deep within the cell (5, 7).

This work was supported by National Institutes of Health Grants AI093533, HL129795, CA016672, EY012128, and EY007551; Cancer Prevention Research Institute of Texas Grant RP110166; and Mexican National Council for Science and Technology Ph.D. Grant Scholarship 448085. The authors declare that they have no conflicts of interest with the contents of this article. The content is solely the responsibility of the authors and does not necessarily represent the official views of the National Institutes of Health.
This article contains Fig. S1.

[1] Submitted in partial fulfillment of the requirements for a Ph.D. degree from Tecnologico de Monterrey.
[2] To whom correspondence should be addressed: Dept. of Pulmonary Medicine, University of Texas M. D. Anderson Cancer Center, 2121 W. Holcombe Blvd., Houston TX 77030. Tel.: 713-563-0410; Fax: 713-563-0411; E-mail: radachi@mdanderson.org.

[3] The abbreviations used are: MC, mast cell; A, cell profile area; cKO, conditional KO; DNP, 2,4-dinitrophenol; fF, femtofarad; Flp, Flp recombinase; GTPγS, guanosine 5′-3-*O*-(thio)triphosphate; HSA, human serum albumin; Neo, neomycin phosphotranferase; PCMC, peritoneal cell-derived MC; PGK, phosphoglucokinase promoter; PI, PMA plus ionomycin; PMA, phorbol 12-myristate 13-acetate; RT-qPCR, reverse transcriptase-quantitative PCR; S, siemens; SM, Sec1/Munc18 family of proteins; SNARE, soluble *N*-ethylmaleimide-sensitive factor attachment protein receptors; Stx, Syntaxin; *Sv*, surface density; VAMP, vesicle-associated membrane protein; *Vv*, volume density.

Most membrane fusion events in eukaryotes are mediated by soluble *N*-ethylmaleimide-sensitive factor attachment protein receptors (SNARE) proteins. The exocytic SNARE proteins include isoforms of synaptosomal-associated protein 25 (SNAP-25), Syntaxin (Stx), and vesicle-associated membrane protein (VAMP), proteins that form a highly stable coiled-coil structure (trans-SNARE complex) that pulls apposing membranes tightly together (8). The formation and function of the SNARE complex requires the intervention of the Sec1 (*Saccharomyces cerevisiae* secretory mutant 1)/Munc18 (mammalian homolog of *Caenorhabditis elegans* uncoordinated gene 18) (SM) family of proteins (9). Among the seven mammalian SM proteins, Munc18-1, -2, and -3 (encoded by the Stx-binding protein/*Stxbp1*, *Stxbp2*, and *Stxbp3* genes) participate in several steps of exocytosis. Munc18 locks Stx into a "closed" conformation preventing the formation of productive trans-SNARE complexes (10, 11). Afterward, interactions with Munc13 catalyze the transition of Stx to an open conformation (12, 13) and promotes binding of Stx's SNARE domain with those of SNAP-25 and VAMP (12, 14). Then Munc18 binds to the N-terminal peptide of Stx (15, 16). This enables the interaction of Munc18 with the trans-SNARE complex to further stabilize it and facilitate efficient membrane fusion (17, 18). In some forms of exocytosis this process is also controlled by Ca^{2+} sensors such as Synaptotagmin (19).

We have shown that Synaptotagmin-2 and Munc13-4 control regulated exocytosis in MCs (20, 21), but the role of Munc18 proteins in MC regulated exocytosis has not been studied in mature MCs. We found that cultured RBL-2H3 cells (a rat basophilic leukemia cell line) express the three Munc18 isoforms (22). Disagreement exists on the role of Munc18-1 in MCs: some could not document expression of Munc18-1 in RBL-2H3 cells (23), others found expression and a functional role of Munc18-1 in degranulation of RBL-2H3 cells (24, 25), and others observed that the absence of Munc18-1 had no effects in fetal liver-derived MCs (26).

Overexpression and knockdown of Munc18-2 in RBL-2H3 cells inhibited degranulation (23, 24, 27). We found that bone marrow-derived MCs from a Munc18-2 hypomorphic mutant mouse had a partial defect in regulated exocytosis (28). However, the extent of the dependence of MC exocytosis on Munc18-2 has not been tested, given that it has never been completely deleted before. Munc18-3 regulates exocytosis in several immune (29–31) and nonimmune cells (32–34). Taking into account that Munc18-3 interacts almost exclusively with Stx4 (35–37) and that Stx4 participates in MC cell degranulation (38–43), it was postulated that Munc18-3 could play a role in MC exocytosis, but this role has yet to be examined. Finally, the role of any Munc18 protein in compound exocytosis has not been explored.

Given these controversies and knowledge gaps and the fact that findings in cell lines sometimes are not reproduced in mature MCs (20, 44), we decided to study the three Munc18 proteins in fully developed MCs to determine whether their functions are supplementary, additive, or antagonistic to each other in the control of MC-regulated exocytosis. We conditionally deleted all three isoforms in MCs and observed a failure in regulated exocytosis only in Munc18-2–deficient MCs. The defect was severe—no exocytosis, single or compound, could be detected in mutant MCs—but it did not affect MC differentiation, number, distribution, or granule biogenesis. Finally, these abnormal MC responses had prominent effects on the reactions of mutant mice to systemic anaphylaxis.

Results

Deletion of Munc18 isoforms in MCs

Using RT-qPCR, we detected expression of the three Munc18 isoforms in mature peritoneal MCs from C57BL/6J mice. Munc18-2 was the predominant isoform (Fig. 1*A*). To study the function of these three proteins in MC exocytosis, we deleted them selectively in MCs using the Cre-loxP system. We obtained Munc18-1 and Munc18-2 cKO mouse lines and created a Munc18-3 cKO line. We flanked exon 1 of the mouse *Stxbp3* gene with two loxP sites (F allele). Removal of this exon by Cre recombinase eliminated the start codon and expression of the protein (Fig. 1*B*). We crossed Munc18-$1^{F/F}$, Munc18-$2^{F/F}$, and Munc18-$3^{F/F}$ mice with B6.C-Tg(CMV-cre)1Cgn/J mice to generate germ-line deletants (− allele) and with Tg(Cma1-cre)ARoer mice (45) to generate MC-specific KO mice (Δ allele). Cre-mediated recombination in the latter line is highly efficient in connective tissue MCs, including peritoneal MCs (21, 45). All mice were genotyped by PCR (Fig. 1*C*). The global deletion of Munc18-1 (46) and of Munc18-2[4] are lethal. Our Munc18-$3^{-/-}$ mice were also not viable: multiple crosses among Munc18-$3^{+/-}$ mice produced 171 mice; 35% were Munc18-$3^{+/+}$, 65% were Munc18-$3^{+/-}$, and none was Munc18-$3^{-/-}$. Munc18-$3^{+/-}$, Munc18-$3^{F/F}$, and Munc18-$3^{\Delta/\Delta}$ mice were fertile, had no gross anatomical abnormalities, and had a normal life span in a barrier facility. We used heterozygotes for the three genes to test for haploinsufficiency.

RT-qPCR from freshly isolated peritoneal MCs from Munc18-2 and -3 mutant mice showed comparable expression between F/F and +/+ animals and complete deletion in Δ/Δ mice. Also, deletion of these two paralogs did not interfere with the expression of the other Munc18 isoforms (Fig. S1). Immunoblots from peritoneal cell-derived MCs (PCMCs) showed that introduction of the loxP sequences did not alter expression of any Munc18 protein in the three F/F lines compared with +/+ controls (Fig. 1, *D–F*). Also, all three Δ/Δ mouse lines lacked expression of the targeted Munc18 gene only in MCs, but in other tissues its expression was comparable with that of the corresponding F/F littermates. The disappearance of the immunoblot bands in Δ/Δ MCs proved the specificity of the three antibodies.

Effects of Munc18 proteins on MC exocytosis

The fact that MCs express the three Munc18 isoforms provided the opportunity to test their functions simultaneously in one system and to determine whether their roles are unique or redundant. The membrane capacitance (C_m) of a cell is proportional to its surface area, which increases as the secretory vesicle membrane is incorporated into the plasma membrane during exocytosis (47, 48). We obtained time-resolved C_m measure-

[4] B. F. Dickey, personal communication.

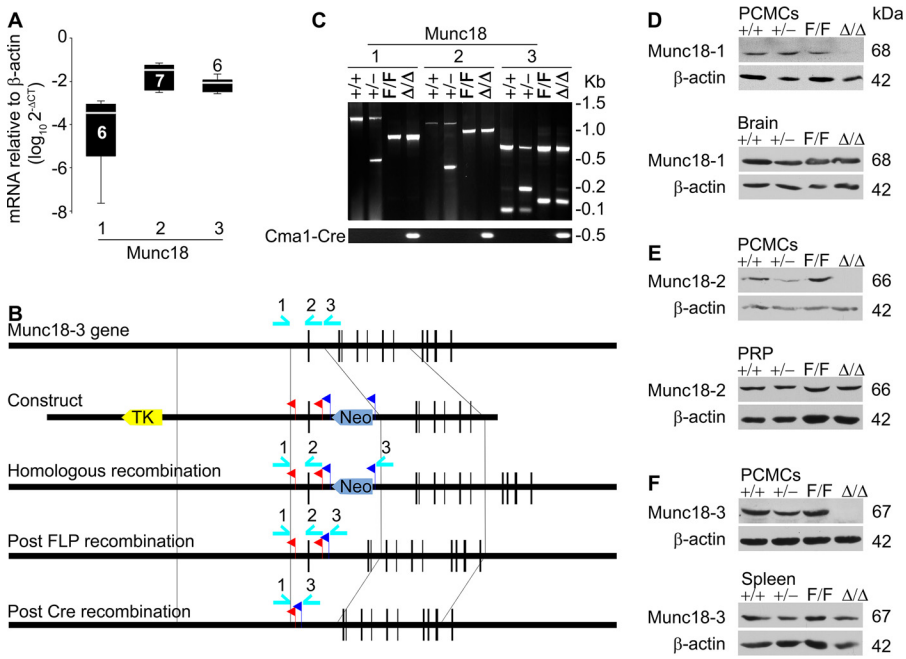

Figure 1. Expression of Munc18 isoforms in MCs. *A*, RT-qPCR from C57BL/6J peritoneal MCs for the three Munc18 paralogs relative to β-actin (ΔCT). *Numbers inside boxes*, number of mice; *white line*, mean; *box*, 25th to 75th percentile; *whiskers*, 5th to 95th percentile. *B*, exon 1 of the Munc18-3 gene was flanked by two loxP sites (*red*) via homologous recombination. Herpes simplex virus thymidine kinase (*TK*; *yellow*) was used for negative selection, and neomycin resistance (*Neo*; *light blue*) flanked by two Flp recognition target sites (*blue*) was used for positive selection and then removed by Flp recombination. Exon 1, with the start codon of the gene, was removed by Cre recombination. *Cyan arrows*, positions of PCR primers. *C*, PCR products from genomic tail DNA from each Munc18 genotype (see "Experimental procedures" for the exact size of the diagnostic bands). *D–F*, representative immunoblots for Munc18-1 (*D*), Munc18-2 (*E*), and Munc18-3 (*F*) of lysates of PCMCs and control tissues. *PRP*, platelet-rich plasma.

ments from MCs using the whole-cell patch clamp configuration while stimulating exocytosis by intracellular dialysis of GTPγS and Ca^{2+} (49, 50). The mean intracellular [Ca^{2+}] achieved, as measured with Fura-2, was 410 ± 21 nM (means ± S.E.). The baseline C_m of all the MCs studied was 6.0 ± 0.3 pF. There were no differences among all genotypes in these two values. We used the gain of C_m over time (Fig. 2, *A–C*) to calculate the total gain in C_m over baseline (ΔC_m) as a measure of the total amount of exocytosis (Fig. 2*G*). We normalized the curves (Fig. 2, *D–F*) and derived the rate of gain between 40 and 60% of total ΔC_m (Fig. 2*H*), which corresponds to the maximum speed of exocytosis. We also recorded the time between cell access and the beginning of the rise in C_m to test whether there was any delay between stimulus and response (Fig. 2, *I* and *J*). Capacitance measurements can also identify individual fusion events, which register as almost instantaneous steps in ΔC_m, with the size of each step proportional to the surface area and thus the volume of each secretory vesicle (5, 47, 48, 51). We measured the amplitudes of the fusion events to determine whether the sizes of the compartments being exocytosed were affected (Fig. 2, *K* and *L*), because a lack of large fusion events correlates with a failure in compound exocytosis (5, 21).

The lack of expression of Munc18-1 (Fig. 2, *A*, *D*, *G*, *H*, *I*, and *K*) or Munc18-3 (Fig. 2, *C*, *F*, *G*, *H*, *J*, and *L*) in MCs did not alter the total amount or speed of exocytosis, the time to initiation of the response, or the size of the vesicles fusing with the plasma membrane. Although we saw no differences among Munc18-$2^{+/+}$, Munc18-$2^{+/-}$, and Munc18-$2^{F/F}$ MCs, the deletion in Munc18-$2^{\Delta/\Delta}$ MCs had a profound effect. These cells barely increased their C_m after activation (Fig. 2, *B* and *G*), and what little they gained was at a very low speed (Fig. 2, *E* and *H*). The defect was so severe that we could not determine the interval to exocytosis because we could not detect an exocytic burst (21). Also, the number of steps recorded from Munc18-$2^{\Delta/\Delta}$ MCs was not enough to obtain a reliable distribution histogram of their sizes, but all of the few steps we observed were ≤8 fF, which corresponds to the size of single granule fusion events, suggesting that compound exocytosis could be affected. After we found that Munc18-1 and -3 were not functionally required for exocytosis in MCs, we continued our studies using only the Munc18-2 mutants.

Effects of Munc18-2 on MC ultrastructural changes dependent on exocytosis

The whole-cell patch clamp configuration cannot detect intracellular fusion events; therefore we turned to the analysis of ultrastructural changes on stimulated MCs by EM and stereology (21). Others have previously reported that the plasma membrane of MCs undergoing degranulation increases its area and complexity (6), their granules increase in volume and lose electron density because of hydration and release of dense core material (52), and as granules fuse with each other inside the cell, they lose their membrane boundaries and create large compound compartments (5).

Five min after activation with phorbol 12-myristate 13-acetate (PMA) and ionomycin (53), all these changes were evident in MCs from every genotype except Munc18-$2^{\Delta/\Delta}$, which were indistinguishable from unstimulated Munc18-$2^{+/+}$ MCs (Fig. 3*A*). We then quantified these changes. First, we created a relative electron-lucency scale, where the greyness of the granules

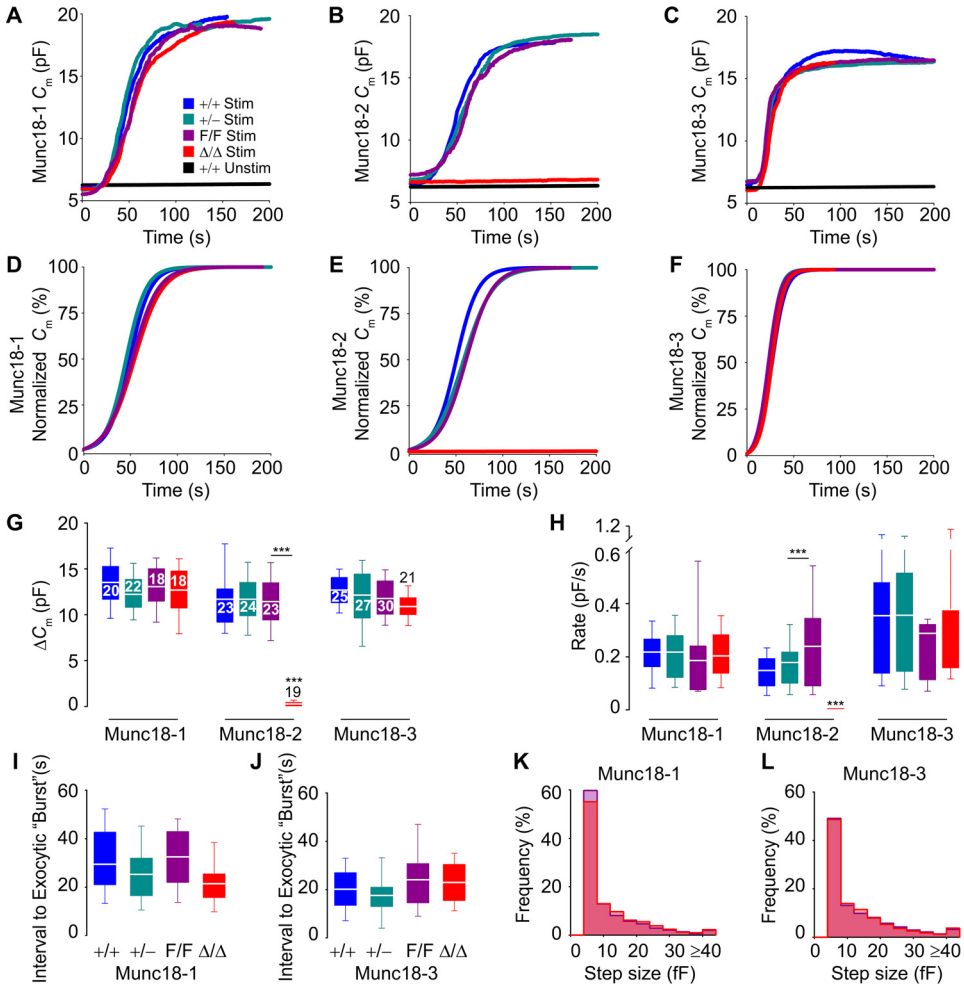

Figure 2. Electrophysiological assessment of MC exocytosis. Single peritoneal MCs from different Munc18-1, Munc18-2, and Munc18-3 mutants were stimulated (*Stim*) by intracellular dialysis of GTPγS and Ca^{2+}. Unstimulated (*Unstim*) +/+ MCs were dialyzed with a GTPγS-free intracellular solution. Access to the cell interior was obtained via establishment of the whole-cell recording configuration at time 0. *A–F*, representative (*A–C*) and normalized (*D–F*) time-resolved capacitance (C_m) traces from Munc18-1 (*A* and *D*), Munc18-2 (*B* and *E*), and Munc18-3 (*C* and *F*) mutant MCs. *Color legend* in *A* applies to all panels. *G* and *H*, average total C_m gain (ΔC_m) (*G*) and rate of ΔC_m between 40 and 60% of total ΔC_m (*H*) from all mutant MCs. *I* and *J*, interval between start of dialysis of GTPγS and Ca^{2+} and beginning of the exocytic burst. The few fusion events recorded from Munc18-$2^{\Delta/\Delta}$ MCs did not meet criteria to identify an exocytic burst. *K* and *L*, frequency distribution of C_m step sizes between 1 and 15% of total ΔC_m. Signals of <4 fF have been removed for clarity. There were not enough events from Munc18-$2^{\Delta/\Delta}$ MCs to perform an analysis. *Number inside boxes* in *G*, number of cells studied, obtained from five to nine animals of each genotype, applies to *G–L*; *white line*, mean; *box*, 25th to 75th percentile; *whiskers*, 5th to 95th percentile. *, $p \leq 0.05$; ***, $p \leq 0.001$; all compared with +/+ unless otherwise specified.

was compared with a scale unique for every cell profile, ranging from the most electron-dense material in the cell (value 0) to the lightness of the extracellular space (value 150). In these individual scales, all granules fell in the 0–120 range, and we used these values to generate a frequency distribution of granule lucencies. Granules from activated Munc18-$2^{+/+}$ MCs were widely distributed, whereas those from stimulated Munc18-$2^{\Delta/\Delta}$ MCs had a narrow left-shifted distribution, almost identical to that of control unstimulated Munc18-$2^{+/+}$ MCs (Fig. 3*B*). When we quantified the volume density (*Vv*) of hypodense granules (electron lucency ≥ 60), they were present in Munc18-2-sufficient MCs but almost absent in Munc18-2–deficient MCs, to a level similar to that of unstimulated WT controls (Fig. 3*C*). As the radius of a sphere increases, its surface-to-volume ratio (quantified as surface density; *Sv*) decreases. The reduction in the *Sv* of the granules of Munc18-$2^{+/+}$ MCs after activation indicates an increase in the size of their granules (swelling), a change that was absent in Munc18-$2^{\Delta/\Delta}$ MCs (Fig. 3*D*). Also missing from Munc18-2–deficient MCs were intracellular compound multivesicular compartments (Fig. 3*E*). Finally, the failure to add plasma membrane area via exocytosis explains the lack of increase in *Sv* of the cell in the absence of Munc18-2 (Fig. 3*F*). All these results confirm that Munc18-2 is required for MC exocytosis and extends this requirement to compound exocytosis.

Effects of Munc18-2 on MC degranulation

Next, to prove that the electrophysiologic changes we observed in the absence of Munc18-2 correspond to a defect in MC degranulation, we evaluated the secretion of mediators stored in MC granules: β-hexosaminidase and histamine (54). PCMCs were sensitized with a specific IgE and then exposed to the antigen (DNP) or PMA and ionomycin (PI). In Munc18-$2^{+/+}$, Munc18-$2^{+/-}$, and Munc18-$2^{F/F}$ MCs, we obtained the expected bell-shaped dose-response curve of released β-hexosaminidase to increasing doses of allergen, whereas Munc18-

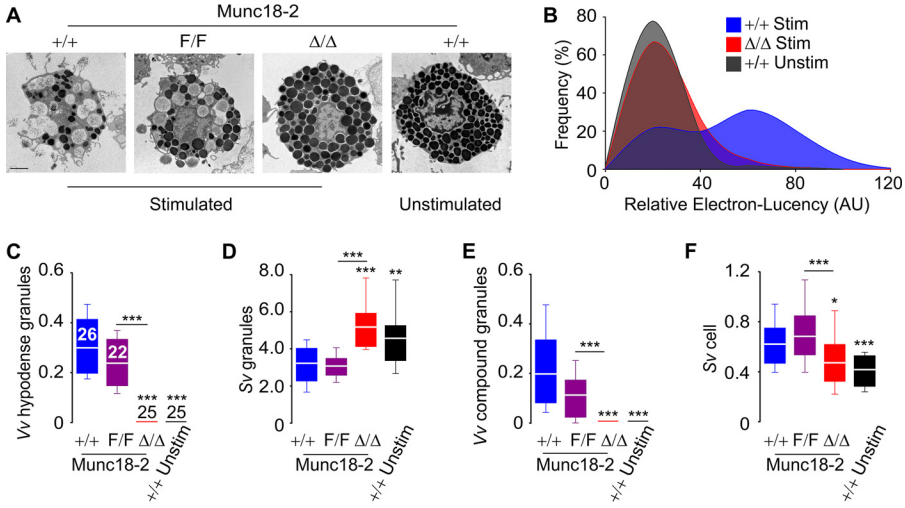

Figure 3. Ultrastructural assessment of MC exocytosis. Peritoneal MCs were stimulated with PMA–ionomycin (*Stim*) or left unstimulated (*Unstim*) and then studied under EM. *A*, representative cell profiles. *Scale bar*, 2 μm. *B*, frequency distribution of electron lucency of MC granules based on a relative scale. *C–F*, stereology of MC profiles: *Vv* of hypodense granules with relative electron lucency ≥ 60 (*C*), *Sv* of granules (*D*), *Vv* of compound granules (*E*), and *Sv* of cells (*F*). *Numbers inside boxes* in *C*, number of cells studied, obtained from three animals of each genotype, applies to *B–F*; *white line*, mean; *box*, 25th to 75th percentile; *whiskers*, 5th to 95th percentile. *, $p \leq 0.05$; **, $p \leq 0.01$; ***, $p \leq 0.001$; all compared with +/+ stimulated MCs unless otherwise indicated.

$2^{\Delta/\Delta}$ MCs exhibited a flat response (Fig. 4*A*). The almost absent secretion observed in Munc18-$2^{\Delta/\Delta}$ MCs was not rescued by using PI as a stronger stimulus (Fig. 4*B*) and was confirmed when we measured secretion of histamine (Fig. 4*C*).

Characterization of Munc18-2–deficient MCs

We had two objectives: to determine whether a structural abnormality and not a pure functional exocytic defect could explain the strong phenotype observed in MCs lacking Munc18-2 and to establish whether an alteration in MC number, distribution, or development could affect the results of our *in vivo* studies. Fluorescence microscopy of ear sections stained with FITC–avidin were used to obtain the density of dermal MCs among all Munc18-2 genotypes, and no differences were noted (Fig. 5*A* and Table 1). In cytospins of peritoneal lavages, we found the same fraction and number of MCs (Table 1), which had similar gross morphology and metachromasia (Fig. 5*B*). EMs of freshly harvested peritoneal MCs were obtained (Fig. 5*C*), and our stereological analysis (Table 1) revealed no differences in *Vv* and *Sv* of granules. The simultaneous constancy of these two values is only possible if the number and size of granules is unaffected. There were also no differences in cell profile area and *Sv* of the cells, indicating that the size and surface complexity of the MCs were similar at rest. In flow cytometry, we identified MCs as double-positive $CD117^+$/$Fc\epsilon RI\alpha^+$ cells. The fractions of MCs in peritoneal lavages (Fig. 5*D*) and in PCMCs after 2 weeks in culture media enriched with IL3 and SCF (Fig. 5*E*) were similar, and the expression levels of these two receptors on the surface of these MCs were almost identical (Table 1). Overall, the level of expression of Munc18-2 did not affect the ultrastructure and number of MCs or their expression of receptors important for their development and activation.

Passive systemic anaphylaxis

It is postulated that MC degranulation plays a central role in anaphylaxis (55). Therefore, we tested the consequences of the MC exocytic abnormalities we identified above in a model of anaphylaxis. We chose passive sensitization because this model depends on IgE, MCs, and histamine (56). In this model, loss of body heat correlates with the severity of the anaphylactic response (57); thus we recorded the drop in body core temperature after systemic allergen challenge (Fig. 6*A*). The lack of response in MC-deficient $Kit^{W\text{-}sh/W\text{-}sh}$ mice confirmed the MC-dependence of this reaction. Our most impressive finding was a markedly reduced response in Munc18-$2^{\Delta/\Delta}$ mice at early (Fig. 6*B*) and late (Fig. 6*C*) time points when compared with all other genotypes. This blunted response correlated with an almost absent histological evidence of MC degranulation in connective tissues (Fig. 6, *D* and *E*) and with a pronounced reduction in circulating histamine after the antigen challenge (Fig. 6*F*). The less severe anaphylactic response, faster recovery, and decreased number of degranulated MCs in tissues in the Munc18-$2^{\Delta/\Delta}$ mice all correlated with our functional and morphological findings on defective MC regulated exocytosis in Munc18-2–deficient MCs.

Discussion

We found that mature peritoneal MCs express all three Munc18 isoforms. The low level of expression of Munc18-1 in MCs (Fig. 1) could explain why some investigators failed to detect it in cell cultures (23). Although three other groups showed that MC lines express Munc18-1 (24–26), they observed opposite effects of this protein on secretion. In one study, fetal liver-derived MCs cells activated via FcεRI did not have any impairment in degranulation in the absence of Munc18-1 (26). Others showed that the knockdown of Munc18-1 expression in RBL-2H3 cells negatively affected degranulation and that expression of Munc18-1 rescued the severe secretory defect in Munc18-1/-2 double-knockdown RBL-2H3 cells (24). A third study showed that the positive effect of Munc18-1 on RBL-2H3 exocytosis depends on its phosphorylation by PKC (25). Although Munc18-1 may control exocytosis in this cell line, given that we observed no exocytic

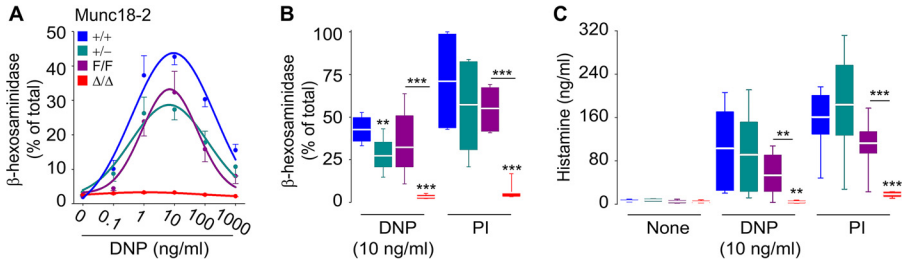

Figure 4. Release of MC secretory contents. PCMCs were sensitized with anti-DNP IgE and challenged with DNP–HSA (DNP) or PI. *A*, β-hexosaminidase released after challenge with different doses of DNP. *B*, β-hexosaminidase released after exposure to DNP or PI (50 ng/ml of PMA plus 1 μM of ionomycin). *C*, histamine released in the absence or presence of DNP or PI. $n = 8$ animals of each genotype. *Circle* and *white line*, mean; *error bar*, S.E.; *box*, 25th to 75th percentile; *whiskers*, 5th to 95th percentile. *, $p \leq 0.05$; **, $p \leq 0.01$; ***, $p \leq 0.001$; all compared with +/+ unless otherwise indicated.

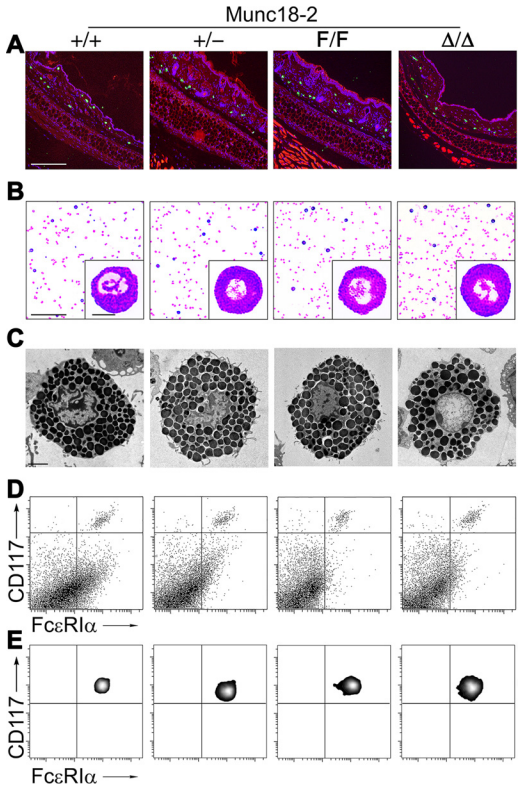

Figure 5. Analysis of MCs in mutant mice. Representative images are shown, for detailed quantification please refer to Table 1. *A*, fluorescence microscopy of ear sections stained with FITC–avidin (*green*) and Hoechst (*blue*); autofluorescence in the *red channel* defined the dermis. *Scale bar*, 200 μm. *B*, cytospins of peritoneal lavages stained with Wright–Giemsa with representative MC (*insets*). *Scale bar*, 200 μm; *inset scale bar*, 10 μm. *C*, EM profiles of resting peritoneal MCs. *Scale bar*, 2 μm. *D* and *E*, flow cytometry of peritoneal MCs (*D*) and PCMCs (*E*) labeled with antibodies against CD117 and FcεRIα.

abnormality in mature MCs lacking Munc18-1 using an extremely sensitive method (Fig. 2), we conclude that this isoform is not required for exocytosis in fully developed MCs.

The potential role for Munc18-3 in MC exocytosis was only hypothetical and was based on: (*a*) the high level of expression of Munc18-3 in MCs (Fig. 1); (*b*) the high affinity of Munc18-3 for Stx4 (36, 37, 58); (*c*) the proven role of this interaction in exocytosis in other cells (29, 36, 59–63); (*d*) the interaction of Stx4 with other exocytic SNARES in RBL-2H3 cells (41, 64); and (*e*) the finding that altering the expression levels of Stx4 in RBL-2H3 cells (38, 41) and MCs (39, 40) modified their degranulation upon activation. Notwithstanding all that, we found that exocytosis is independent of Munc18-3 in mature MCs (Fig. 2) and conclude that this protein is dispensable for MC degranulation.

Given the discordant results on the roles of Synaptotagmin-2 (20, 44) and Munc18-1 (see above) obtained from RBL-2H3 cells *versus* mature MCs, we consider it important to study Munc18-2 in fully developed MCs. Also, although there was previous evidence that lowering expression levels of this protein decreases degranulation in RBL-2H3 cells (24, 27, 65), bone marrow-derived MCs (28, 65), and mature MCs (28), the only approach to evaluate the degree of dependence of this process on this protein is the complete removal of Munc18-2 from the system. Different from the partial exocytic defect that we observed in Synaptotagmin-2–deficient (20) and Munc13-4–deficient MCs (21), there was almost no residual exocytosis after deleting Munc18-2 by electrophysiologic (Fig. 2) and morphologic (Fig. 3) criteria. Moreover, this defect was entirely functional and not a consequence of morphologic abnormalities in the mutant MCs (Fig. 5 and Table 1). Munc18-1 can interact with many of the Stxs proven to be functional partners of Munc18-2 (36, 66, 67), and it has been shown recently that Munc18-3 can bind to Stxs other than Stx4 *in vitro* (68), suggesting that Munc18-1 and -3 could compensate for the loss of Munc18-2. Nevertheless, we found an almost complete failure in exocytosis in mature MCs lacking Munc18-2 despite almost normal expression levels of Munc18-1 and -3 in these mutant MCs (Fig. S1), indicating that Munc18-1 and -3 do not play any role in MC exocytosis *in vivo*, not even a redundant one.

The residual exocytosis observed in MCs lacking Munc13-4 allowed us to document a significant delay between stimulus and response, and we interpreted that as a failure in vesicle priming (21). Because there were very few exocytic events in the absence of Munc18-2, we could not reliably perform this analysis. Therefore, we cannot draw any conclusions on the role of Munc18-2 in vesicle priming in MCs.

It has been estimated that the fusion of a single MC granule with the plasma membrane should increase its C_m by ~7 fF (69). The analysis of the C_m step sizes in Munc13-4$^{\Delta/\Delta}$ MCs showed that the residual exocytosis was comprised mostly of steps of ≤8 fF, indicating that the small remaining response was mainly dependent on single-vesicle exocytosis (21). In the case of Munc18-2 deficiency, the scarcity of fusion events made it impossible to perform a formal distribution analysis, but no event of >8 fF was noted, suggesting a defect in compound exocytosis (5). Three possible explanations were that in the absence of Munc18-2 there is a failure in granule biogenesis,

Table 1

Characterization of MCs from mutant Munc18-2 mice

The results are means ± S.E. from five mice of each genotype unless otherwise specified. A, cell profile area; AU, arbitrary units; MFI, mean fluorescence intensity. No significant differences were found among mice of all genotypes in any category.

	Munc18-2$^{+/+}$	Munc18-2$^{+/-}$	Munc18-2$^{F/F}$	Munc18-2$^{\Delta/\Delta}$
Dermal MCs				
Density (cells/mm^2 of dermis)[a]	186 ± 45	178 ± 73	157 ± 38	166 ± 18
Peritoneal MCs				
Count (cells/μl)[b]	28 ± 8	18 ± 5	19 ± 1	24 ± 6
MCs (%)[b]	3.6 ± 0.4	3.3 ± 0.5	2.7 ± 0.3	2.8 ± 0.3
Vv[c]	0.68 ± 0.02	0.7 ± 0.01	0.7 ± 0.01	0.69 ± 0.01
Sv cell (μm^{-1})[c]	0.4 ± 0.03	0.5 ± 0.02	0.5 ± 0.04	0.5 ± 0.03
Sv granule (μm^{-1})[c]	4.5 ± 0.3	4.9 ± 0.4	4.3 ± 0.1	4.4 ± 0.2
A (μm^2)[c]	74.5 ± 3.0	64.7 ± 2.7	70.3 ± 2.7	70.7 ± 2.3
CD117$^+$/FcεRIα^+ (%)[d]	1.2 ± 0.002	0.9 ± 0.001	1.0 ± 0.001	0.9 ± 0.003
MFI CD117 (AU)[e]	3.8 ± 0.1	3.4 ± 0.3	3.5 ± 0.4	3.0 ± 0.3
MFI FcεRIα (AU)[e]	5.6 ± 0.3	6.4 ± 0.3	6.6 ± 0.4	6.9 ± 0.3
PCMCs				
CD117$^+$/FcεRIα^+ (%)[d]	98.8 ± 0.001	96.7 ± 0.011	97.0 ± 0.012	96.3 ± 0.013
MFI CD117 (AU)[e]	9.5 ± 0.3	9.2 ± 0.3	9.0 ± 0.3	8.2 ± 0.8
MFI FcεRIα (AU)[e]	8.6 ± 0.8	7.0 ± 0.5	8.4 ± 0.7	8.1 ± 0.4

[a] Cells with FITC$^+$ granules and a Hoechst$^+$ nucleus per mm^2 of dermis in random 5-μm sections of ear (8–10 sections/mouse).
[b] Neubauer chamber counts and differentials of cytospins of recovered peritoneal lavage (n = 7–12 mice; 1 sample per mouse).
[c] Stereological analysis of randomly acquired EM images of peritoneal MCs (25 cell profiles, 3 mice/genotype).
[d] Fraction of CD117$^+$/FcεRIα^+ double-positive cells in peritoneal MCs or PCMCs by flow cytometry (1 sample/mouse).
[e] Cell surface expression of CD117 and FcεRIα expressed as MFI of specific labeled primary antibodies (1 sample/mouse).

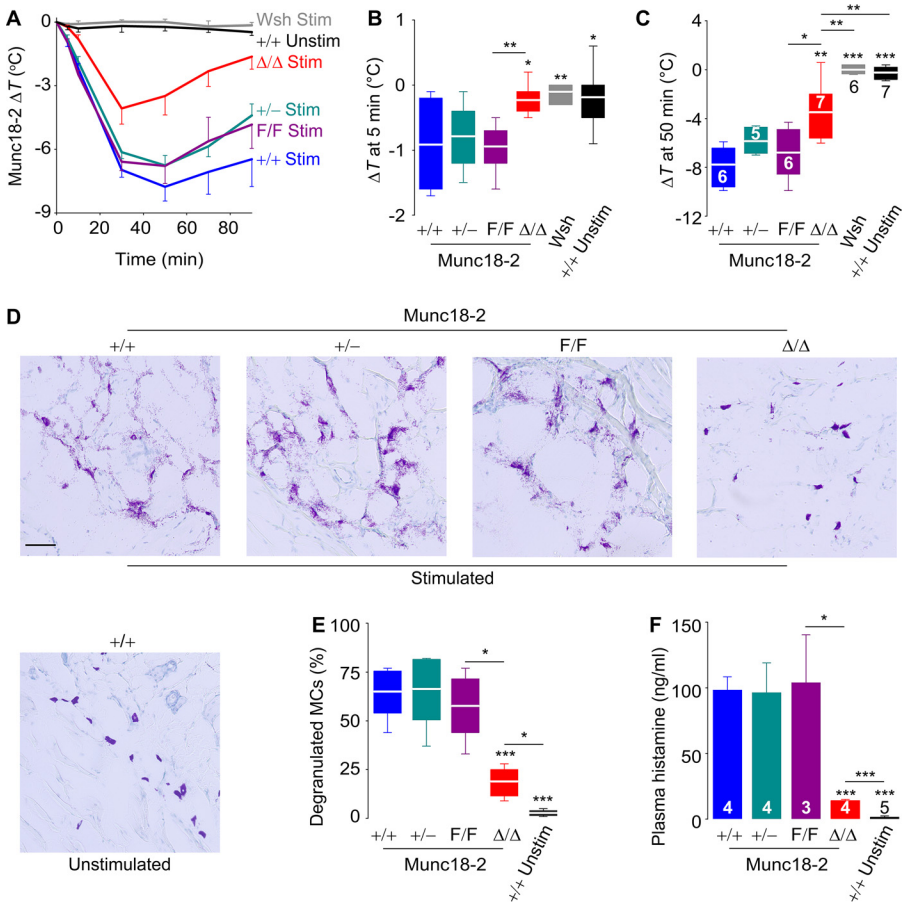

Figure 6. Passive systemic anaphylaxis. MC-deficient Kit$^{W\text{-}sh/W\text{-}sh}$ (*Wsh*) and Munc18-2 mutant mice were sensitized with anti-DNP IgE intraperitoneally and challenged (*Stim*) 24 h later with DNP–HSA intraperitoneally. *Unstim*, mice sensitized but not challenged. *A*, change in body core temperature (ΔT) after challenge. *B* and *C*, ΔT 5 min (*B*) and 50 min (*C*) after challenge. *Number inside boxes in C*, number of mice, applies to *A–C* and *E*. *D*, representative lip sections stained with toluidine blue 90 min after challenge. *Scale bar*, 100 μm. *E*, fraction of degranulated MCs in lip sections. *F*, plasma histamine 15 min after challenge. *Number inside bars* in *F*, number of mice. *Line*, *white line*, and *bar*, mean; *error bar*, S.E.; *box*, 25th to 75th percentile; *whiskers*, 5th to 95th percentile. *, $p \leq 0.05$; **, $p \leq 0.01$; ***, $p \leq 0.001$; all compared with +/+ stimulated mice unless otherwise indicated.

that fusion between granules was impaired, and that intergranular fusion was taking place, but the resulting large multivesicular compound compartments were unable to fuse with the plasma membrane. Because C_m recordings are unable to distinguish among these options, we drew upon EM analysis of resting (Table 1) and activated (Fig. 3) MCs. Once again, stere-

ology of profiles of activated MCs proved to be an excellent complement to MC electrophysiology (21). We observed that although the MC granules were normal in size and number, there was an almost total failure in granule-to-granule fusion. Hence, like Munc13-4, Munc18-2 is required for the heterotypic fusion of vesicle to plasma membrane and the homotypic fusion between vesicle membranes, and consequently it controls both single-vesicle and compound exocytosis.

The failure in MC degranulation in the absence of Munc18-2 documented *in vitro* was confirmed *in vivo* when we observed a marked reduction in plasma histamine levels and histologic markers of MC degranulation in Munc18-$2^{\Delta/\Delta}$ mice subjected to a model of systemic anaphylaxis (Fig. 6). Relative to WT controls, the loss in hypothermic response in this model is more complete in Munc18-$2^{\Delta/\Delta}$ mice (Fig. 6) than in Munc13-$4^{\Delta/\Delta}$ mice (21). We think that the more severe defect in exocytosis in the absence of Munc18-2 (the residual exocytosis observed in Munc13-$4^{\Delta/\Delta}$ MCs was not present in Munc18-$2^{\Delta/\Delta}$ MCs) accounts for the difference.

On the other hand, compared with controls, the anaphylactic response is significantly decreased but not absent. The residual anaphylactic response in Munc18-$2^{\Delta/\Delta}$ is more likely due to residual MC function than to the participation of other allergic effector cells (*e.g.* basophils and platelets) because MC-deficient mice (70) are completely protected from anaphylaxis (Fig. 6*A*). MCs could be grouped into many subpopulations depending upon different criteria (71). A useful classification (72) distinguishes between constitutive/connective tissue MCs, evolutionarily the most primitive and the most abundant in naïve mammals (73), and inducible/mucosal MCs, which depend on T-cell–derived cytokines for development (74, 75). Cma1 (mMCP-5) is expressed mainly in the former (71, 76, 77). Hence, it is possible that a small population of mucosal MCs that do not undergo recombination and do not lose Munc18-2 expression accounts for the weak reaction. Another possibility is that MC responses independent of exocytosis, such as eicosanoid generation, are responsible. In conclusion, MC exocytosis is an important component of the anaphylactic response, and Munc18-2 is the sole, nonredundant Munc18 isoform that mediates both homotypic and heterotypic membrane fusion during MC degranulation.

Experimental procedures

Mice

C57BL/6J (catalog no. 000664), MC-deficient (B6.Cg-*Kit*$^{W\text{-}sh}$/HNihrJaeBsmGlliJ; catalog no. 012861), B6.129S4-*Gt(ROSA)26Sor*$^{tm1(FLP1)Dym}$/RainJ (catalog no. 009086), and B6.C-Tg(CMV-cre)1Cgn/J (catalog no. 006054) mice were purchased from The Jackson Laboratory. We obtained Munc18-1 cKO mice from Dr. Matthijs Verhage (University of Amsterdam) (78), Munc18-2 cKO mice from Drs. Michael J. Tuvim and Burton F. Dickey (University of Texas M. D. Anderson Cancer Center),[5] and Tg(Cma1-cre)ARoer mice from Dr. Axel Roers (University of Cologne) (45).

In the Munc18-1 cKO line, exon 2 of *Stxbp1* is flanked by two loxP sites, and the frameshift induced by Cre recombination results in nonsense mutations and absence of the protein (78). In the Munc18-2 cKO mouse, the targeted exon was exon 1, and recombination removes the translation initiation codon.[4] To create a Munc18-3 cKO by homologous recombination, we built a targeting vector to insert a loxP upstream of exon 1 (GRCm38; Chr3:1088440680) of the mouse *Stxbp3* gene and a second loxP followed by the phosphoglucokinase promoter-neomycin resistance gene (PGK–Neo) flanked by two Flp recognition target sites in intron 1 (Chr3:108840293–108840125). The herpes simplex virus thymidine kinase gene was introduced outside the homology arms (Fig. 1*B*). The construct was electroporated into C57BL/6 ES cells, and genetically modified mice were created as described (21). The mutant mice were crossed with B6.129S4-*Gt(ROSA)26Sor*$^{tm1(FLP1)Dym}$/RainJ mice to remove PGK–Neo, leaving exon 1 flanked by two loxP sites (F allele). We crossed Munc18-$1^{F/F}$, Munc18-$2^{F/F}$, and Munc18-$3^{F/F}$ mice with B6.C-Tg(CMV-cre)1Cgn/J CMV-Cre to delete the targeted gene in the germ line and produce global heterozygote (+/−) lines, and with Tg(Cma1-cre)ARoer mice to generate MC-specific deletant mice (Δ/Δ) (21, 45).

Genotyping was done by PCR. We modified the published strategy for Munc18-1 using the following primers: primer 1, 5′-CCTGTATGGGTACTGTTCGTTCACTAAAATA-3′; primer 2, 5′-GCACAAAAGTGTTCTATCCTGCAGAGTT-3′; primer 3, 5′-TTCTGAACTTGAGGCCAGTCTGAGACA-CAG-3′; and primer 4, 5′-TTGGTGGTCGAATGGGCAGG-TAG-3′. Primers 1 and 2 produced bands for the + allele (1680 bp) and the − allele (520 bp). Primers 1, 3, and 4 produced bands for the + allele (190 bp) and F allele (1000 bp). For Munc18-2 the primers were: primer 1, 5′-GCAAAGGAGAG-AGAGAGAGCC-3′; primer 2, 5′-GGGTGCTCATACAATA-CGTGG-3′; primer 3, 5′-CAGTTGGTCAAATTCAAGTG-CTC-3′; and primer 4, 5′-AAGGCGGTGGTAGGGGAAAGT-3′. Primers 1 and 2 produced bands for the + allele (1178 bp) and the − allele (478 bp). Primers 3 and 4 produced bands for the + allele (931 bp) and the F allele (1075 bp). For Munc18-3 the primers were: primer 1, 5′-TATAGTAGGCTTCCGCTA-GGG-3′; primer 2, 5′-TCACGCGCATCAACTAGG-3′; and primer 3, 5′-TGTGTCGGATGGAGAGACG-3′, which produced distinct bands for the + allele (107 bp), the F allele (153 bp), and the − allele (225 bp). The presence of genomic Cre was detected as described (21). All experiments used littermates as controls. All lines were on a C57BL/6 background, as confirmed by speed-congenic scanning for 105 SNPs. All experiments were carried out using animal protocols approved by the Institutional Animal Care and Use Committee of the University of Texas M. D. Anderson Cancer Center.

MC harvest, culture, flow cytometry, and FACS

Peritoneal MCs were harvested and processed as described (21, 79). Briefly, peritoneal lavage cells were counted in a Neubauer chamber and in cytospins stained with Wright-Giemsa. For PCMCs, peritoneal cells were kept in complete medium (Iscove's modified Dulbecco's medium with glutamine, 10% FBS, 500 units/ml penicillin, 500 units/ml streptomycin, 1× vitamins, 1× nonessential amino acids, 100 μM sodium pyruvate, 50 μM 2-mercapthoethanol; Thermo Fisher) with 5 ng/ml rmIL3 (Peprotech) and 10 ng/ml rmSCF (R & D Systems) for 2

[5] M. J. Tuvim and B. F. Dickey, manuscript in preparation.

weeks (37 °C, 5% CO_2, biweekly media changes). For flow cytometry, 10^6 peritoneal lavage cells or PCMCs were blocked with anti-mouse CD16/CD32 and labeled with phycoerythrin-cyanine-7 anti-mouse CD117 and allophycocyanin anti-mouse FcεRIα antibodies (all from BD Biosciences) and then analyzed, recording the number of double-positive $CD117^+$/FcεRIα^+ cells and their mean fluorescence intensity in each channel. To isolate MCs from peritoneal lavages by FACS, the cells were labeled as above, and the double-positive ones were sorted.

Expression analyses

For RT-qPCR, sorted peritoneal MCs were lysed, RNA was extracted (RNeasy mini kit; Qiagen) and reverse-transcribed (qSCRIPT cDNA SuperMix; Quantabio). qPCR of each cDNA sample was performed with qPCR master mix (Quantabio) and fluorescein amidite-labeled probes for β-actin (Mm02619580_g1), Munc18-1 (Mm00436837_m1), Munc18-2 (Mm00441589_m1), and Munc18-3 (Mm00441605_m1; all from Thermo Fisher Scientific) in triplicate on a ViiA 7 RT-PCR System (Applied Biosystems). The results were expressed as $\Delta\Delta Ct$ (normalized for β-actin and then for levels in WT controls). For immunoblots, the samples were sonicated and lysed (21). The lysates were run under denaturing conditions in 10% polyacrylamide gels and transferred to nitrocellulose membranes. The samples were probed with polyclonal rabbit antibodies against Munc18-1 (1:4,000), Munc18-2 (1:200), Munc18-3 (1:5,000; all from Sigma–Aldrich), and β-actin (1:20,000; loading control; Abcam).

Histology

The ears were processed as described (28). In brief, 5-μm cross-sections embedded in paraffin were stained with 2.5 mg/ml of FITC–avidin and 20 mM Hoechst (both from Thermo Fisher) for 1 h at room temperature. Cells with $FITC^+$ granules surrounding a $Hoechst^+$ nucleus were counted as MCs. The density of MCs was expressed as number of MCs per mm^2 of dermis, which was delineated as the area between the epidermis and the auricular cartilage or muscle using the autofluorescence of these tissues under a Texas Red filter. For quantification of MC degranulation in tissues, the mice were euthanized 90 min after the anaphylactic challenge. The lips were excised, fixed (0.5% paraformaldehyde, pH 7.0, 4 °C, overnight), and embedded in OCT compound. Sections of 5 μm were stained with toluidine blue (pH 2.0; MP Biomedicals). A MC was classified as degranulated if most (> 50%) of its metachromatic granules were found extracellularly (21).

EM and stereology

5×10^6 peritoneal cells per sample were activated with PMA (20 ng/ml) plus ionomycin (1 μg/ml) in 1 ml of PBS for 5 min at 37 °C. Activation was stopped by adding cold glutaraldehyde (final concentration, 2%) on ice, and then EM samples were handled as described (21). Sections of 100-nm thickness were stained with uranyl acetate and lead citrate and then imaged on a Tecnai 12 transmission electron microscope. MC profiles containing a nuclear profile were recorded. Stereology was performed using a line-segments-and-points grid in STEPanizer (80). Points inside cell profiles and granules and line intercepts with plasma and granule membranes were counted to obtain A, Vv, and Sv (20). Agglomerates of multiple granule profiles not separated by a membrane were counted as multigranular compartments (21). The relative electron lucency of MC granules was computed using an internal scale adjusted for each cell profile. Circles with an area of 0.0366 μm^2 within granules selected randomly with a cycloid grid were digitally graded using a 0–150 point gray scale, where 0 represents the most electron-dense structure in the cell profile, and 150 represents the lightness of the extracellular space. Granules with relative electron lucency of <60 were categorized as dense, and those of ≥60 as were categorized hypodense.

MC secretion assays

Assays were performed as described (21). Briefly, 3×10^4 PCMCs were sensitized with 100 ng/ml of mouse anti-DNP IgE (clone SPE-7; Sigma–Aldrich) for 5 h. They were washed and resuspended in 90 μl of degranulation buffer. Then 10 μl of degranulation buffer containing no extra compounds (negative control) or DNP–HSA (final concentrations 0.1, 1, 10, 100 and 1000 ng/ml) or PMA (final concentration 50 ng/ml) with ionomycin (final concentration, 1 μM) was added. After 30 min, supernatants were collected, and the remaining cells were lysed. For β-hexosaminidase, 50 μl of supernatant or lysates were mixed with 100 μl of 4-nitrophenyl *N*-acetyl-β-D-glucosaminide (3.5 mg/ml) in citrate buffer and incubated at 37 °C for 90 min. The reaction was stopped by adding 100 μl of glycine (pH 10.7; 400 mM). Then the absorbance at $\lambda = 405$ nm was recorded (reference $\lambda = 620$ nm), and β-hexosaminidase activity was reported as a fraction of the total cell content. ELISA (Oxford Biochemicals) was used to measure histamine in supernatants.

Electrophysiology

Whole-cell recordings from individual MCs were made using 3–8 MΩ Sylgard-coated patch pipettes. The internal solution defined intracellular $[Ca^{2+}]$ and induced degranulation and contained 0.05 mM GTPγS, 135 mM potassium gluconate, 10 mM HEPES, 0.1 mM Fura-2, 7 mM $MgCl_2$, 3 mM KOH, 0.2 mM Na-ATP, and either 10 mM K_2 EGTA with 8 mM $CaCl_2$ or 2.5 mM Cs-EGTA with 7.5 mM Ca-EGTA (pH 7.21, 0.304 osmoles) (49, 50, 81). The intracellular $[Ca^{2+}]$ was determined ratiometrically from the emitted Fura-2 fluorescence at two different wavelengths (82–84), and Ca^{2+} calibration constants determined *in vitro* using a multipoint calibration kit (Thermo Fisher Scientific/Molecular Probes) and analyzed in IgorPro (Wavemetrics). For recordings of membrane capacitance (C_m), membrane conductance (G_m), and series conductance (G_s), an 800 Hz sinusoidal, 30 mV peak-to-peak stimulus was applied around a holding potential of −70 mV, and the resultant signal was analyzed using the Lindau–Neher technique (85, 86). For each 100-ms sweep, the average value was recorded, yielding a temporal resolution for C_m, G_m, and G_s of ~7 Hz. Cells selected for analysis met the criteria of $G_m \leq 1{,}200$ pS, $G_s \geq 35$ nS, and steady-state intracellular $[Ca^{2+}] = 400 \pm 100$ nM. The total change in C_m (ΔC_m) was calculated as the difference between the prestimulus baseline and the maximum plateau in C_m. Each trace of C_m over time was fitted to a four-parameter sigmoid

function, normalized to its total ΔC_m and then used to obtain the rates of C_m from 40–60% of total ΔC_m. The exocytic burst was identified as successive step changes in $C_m \geq 8$ fF sustained for >4 s, and the time between whole-cell access and the first fusion event with $C_m \geq 8$ fF within this 4-s region was noted (21). We also measured the sizes of all the steps between 1 and 15% of total ΔC_m after eliminating any signal of <4 fF to decrease noise.

Passive systemic anaphylaxis

The mice were sensitized intraperitoneally with 20 μg of mouse monoclonal anti-DNP IgE in 100 μl of PBS. After 24 h, the mice were challenged intraperitoneally with 1 mg of DNP–HSA in 100 μl of PBS. Body core temperature was monitored using a rectal probe (DT80–1; General). At 90 min, the mice were euthanized, and their lips were processed as described above. Another set of mice were manipulated as above, but 15 min after the challenge, they were anesthetized with isoflurane, and blood was collected via inferior vena cava puncture with a 21-gauge needle into a citrated syringe, slowly and avoiding bubbles to prevent platelet activation. An equal volume of Tyrode's buffer (5.6 mM glucose, 140 mM NaCl, 12 mM $NaHCO_3$, 2.7 mM KCl, and 0.46 mM NaH_2PO_4) was added, plasma was separated by centrifugation, and histamine was measured by ELISA.

Statistical analysis

For continuous variables, we compared the means of all groups by one-way analysis of variance; if a significant difference was detected, we applied Tukey's test for multiple pairwise comparisons, Dunnett's test for multiple comparisons against the control group, and two-tailed unpaired Student's t test for simple comparisons. For categorical data, we used Pearson's χ^2 test or Fisher's exact test. Significance was set at $p < 0.05$.

Author contributions—B. A. G. and R. A. conceptualization; B. A. G., M. A. C., A. I. R., and R. A. software; B. A. G., M. A. C., A. I. R., M. A. R., and R. A. formal analysis; B. A. G., M. A. C., and R. A. validation; B. A. G., M. A. C., A. I. R., M. A. R., A. D., Y. P., A. J. D., R. M. C., R. E., A. R. B., R. H., and R. A. investigation; B. A. G., M. A. C., and R. A. visualization; B. A. G., M. A. C., A. R. B., R.H., and R. A. methodology; B. A. G., B. F. D., and R. A. writing-original draft; B. A. G., A. R. B., R. H., and R. A. writing-review and editing; M. J. T., B. F. D., and R. A. resources; R. A. supervision; R. A. funding acquisition; R. A. project administration.

Acknowledgments—We thank Margaret M. Gondo (University of Houston) for professional assistance with EM and Dr. Thomas C. Südhof for the backbone of the targeting vector.

References

1. Moon, T. C., St Laurent, C. D., Morris, K. E., Marcet, C., Yoshimura, T., Sekar, Y., and Befus, A. D. (2010) Advances in mast cell biology: new understanding of heterogeneity and function. *Mucosal. Immunol.* **3,** 111–128 CrossRef Medline
2. Galli, S. J., and Tsai, M. (2012) IgE and mast cells in allergic disease. *Nat. Med.* **18,** 693–704 CrossRef Medline
3. Berridge, M. J. (1987) Inositol trisphosphate and diacylglycerol: two interacting second messengers. *Annu. Rev. Biochem.* **56,** 159–193 CrossRef Medline
4. Pang, Z. P., and Südhof, T. C. (2010) Cell biology of Ca^{2+}-triggered exocytosis. *Curr. Opin. Cell Biol.* **22,** 496–505 CrossRef Medline
5. Alvarez de Toledo, G., and Fernandez, J. M. (1990) Compound versus multigranular exocytosis in peritoneal mast cells. *J. Gen. Physiol.* **95,** 397–409 CrossRef Medline
6. Röhlich, P., Anderson, P., and Uvnäs, B. (1971) Electron microscope observations on compounds 48–80-induced degranulation in rat mast cells: evidence for sequential exocytosis of storage granules. *J. Cell Biol.* **51,** 465–483 CrossRef Medline
7. Pickett, J. A., and Edwardson, J. M. (2006) Compound exocytosis: mechanisms and functional significance. *Traffic* **7,** 109–116 CrossRef Medline
8. Lin, R. C., and Scheller, R. H. (1997) Structural organization of the synaptic exocytosis core complex. *Neuron* **19,** 1087–1094 CrossRef Medline
9. Südhof, T. C., and Rothman, J. E. (2009) Membrane fusion: grappling with SNARE and SM proteins. *Science* **323,** 474–477 CrossRef Medline
10. Dulubova, I., Sugita, S., Hill, S., Hosaka, M., Fernandez, I., Südhof, T. C., and Rizo, J. (1999) A conformational switch in syntaxin during exocytosis: role of munc18. *EMBO J.* **18,** 4372–4382 CrossRef Medline
11. Misura, K. M., Scheller, R. H., and Weis, W. I. (2000) Three-dimensional structure of the neuronal-Sec1-syntaxin 1a complex. *Nature* **404,** 355–362 CrossRef Medline
12. Ma, C., Li, W., Xu, Y., and Rizo, J. (2011) Munc13 mediates the transition from the closed syntaxin-Munc18 complex to the SNARE complex. *Nat. Struct. Mol. Biol.* **18,** 542–549 CrossRef Medline
13. Yang, X., Wang, S., Sheng, Y., Zhang, M., Zou, W., Wu, L., Kang, L., Rizo, J., Zhang, R., Xu, T., and Ma, C. (2015) Syntaxin opening by the MUN domain underlies the function of Munc13 in synaptic-vesicle priming. *Nat. Struct. Mol. Biol.* **22,** 547–554 CrossRef Medline
14. Lai, Y., Choi, U. B., Leitz, J., Rhee, H. J., Lee, C., Altas, B., Zhao, M., Pfuetzner, R. A., Wang, A. L., Brose, N., Rhee, J., and Brunger, A. T. (2017) Molecular mechanisms of synaptic vesicle priming by Munc13 and Munc18. *Neuron* **95,** 591–607 CrossRef Medline
15. Rathore, S. S., Bend, E. G., Yu, H., Hammarlund, M., Jorgensen, E. M., and Shen, J. (2010) Syntaxin N-terminal peptide motif is an initiation factor for the assembly of the SNARE-Sec1/Munc18 membrane fusion complex. *Proc. Natl. Acad. Sci. U.S.A.* **107,** 22399–22406 CrossRef Medline
16. Shen, J., Rathore, S. S., Khandan, L., and Rothman, J. E. (2010) SNARE bundle and syntaxin N-peptide constitute a minimal complement for Munc18-1 activation of membrane fusion. *J. Cell Biol.* **190,** 55–63 CrossRefMedline
17. Shen, J., Tareste, D. C., Paumet, F., Rothman, J. E., and Melia, T. J. (2007) Selective activation of cognate SNAREpins by Sec1/Munc18 proteins. *Cell* **128,** 183–195 CrossRef Medline
18. Shen, C., Rathore, S. S., Yu, H., Gulbranson, D. R., Hua, R., Zhang, C., Schoppa, N. E., and Shen, J. (2015) The trans-SNARE-regulating function of Munc18-1 is essential to synaptic exocytosis. *Nat. Commun.* **6,** 8852 CrossRefMedline
19. Li, Y., Wang, S., Li, T., Zhu, L., Xu, Y., and Ma, C. (2017) A stimulation function of synaptotagmin-1 in ternary SNARE complex formation dependent on Munc18 and Munc13. *Front. Mol. Neurosci.* **10,** 256 CrossRef Medline
20. Melicoff, E., Sansores-Garcia, L., Gomez, A., Moreira, D. C., Datta, P., Thakur, P., Petrova, Y., Siddiqi, T., Murthy, J. N., Dickey, B. F., Heidelberger, R., and Adachi, R. (2009) Synaptotagmin-2 controls regulated exocytosis but not other secretory responses of mast cells. *J. Biol. Chem.* **284,** 19445–19451 CrossRef Medline
21. Rodarte, E. M., Ramos, M. A., Davalos, A. J., Moreira, D. C., Moreno, D. S., Cardenas, E. I., Rodarte, A. I., Petrova, Y., Molina, S., Rendon, L. E., Sanchez, E., Breaux, K., Tortoriello, A., Manllo, J., Gonzalez, E. A., *et al.* (2018) Munc13 proteins control regulated exocytosis in mast cells. *J. Biol. Chem.* **293,** 345–358 CrossRef Medline
22. Nigam, R., Sepulveda, J., Tuvim, M., Petrova, Y., Adachi, R., Dickey, B. F., and Agrawal, A. (2005) Expression and transcriptional regulation of Munc18 isoforms in mast cells. *Biochim. Biophys. Acta* **1728,** 77–83 CrossRef Medline
23. Martin-Verdeaux, S., Pombo, I., Iannascoli, B., Roa, M., Varin-Blank, N., Rivera, J., and Blank, U. (2003) Evidence of a role for Munc18-2 and

microtubules in mast cell granule exocytosis. *J. Cell Sci.* **116,** 325–334 Medline
24. Bin, N. R., Jung, C. H., Piggott, C., and Sugita, S. (2013) Crucial role of the hydrophobic pocket region of Munc18 protein in mast cell degranulation. *Proc. Natl. Acad. Sci. U.S.A.* **110,** 4610–4615 CrossRef Medline
25. Adhikari, P., and Xu, H. (2018) PKC-dependent phosphorylation of Munc18a at Ser313 in activated RBL-2H3 cells. *Inflamm. Res.* **67,** 1–3 CrossRef Medline
26. Wu, Z., MacNeil, A. J., Berman, J. N., and Lin, T. J. (2013) Syntaxin binding protein 1 is not required for allergic inflammation via IgE-mediated mast cell activation. *PLoS One* **8,** e58560 CrossRef Medline
27. Tadokoro, S., Kurimoto, T., Nakanishi, M., and Hirashima, N. (2007) Munc18-2 regulates exocytotic membrane fusion positively interacting with syntaxin-3 in RBL-2H3 cells. *Mol. Immunol.* **44,** 3427–3433 CrossRefMedline
28. Kim, K., Petrova, Y. M., Scott, B. L., Nigam, R., Agrawal, A., Evans, C. M., Azzegagh, Z., Gomez, A., Rodarte, E. M., Olkkonen, V. M., Bagirzadeh, R., Piccotti, L., Ren, B., Yoon, J. H., McNew, J. A., *et al.* (2012) Munc18b is an essential gene in mice whose expression is limiting for secretion by airway epithelial and mast cells. *Biochem. J.* **446,** 383–394 CrossRef Medline
29. Brochetta, C., Vita, F., Tiwari, N., Scandiuzzi, L., Soranzo, M. R., Guérin-Marchand, C., Zabucchi, G., and Blank, U. (2008) Involvement of Munc18 isoforms in the regulation of granule exocytosis in neutrophils. *Biochim. Biophys. Acta* **1783,** 1781–1791 CrossRef Medline
30. Houng, A., Polgar, J., and Reed, G. L. (2003) Munc18-syntaxin complexes and exocytosis in human platelets. *J. Biol. Chem.* **278,** 19627–19633 CrossRef Medline
31. Schraw, T. D., Lemons, P. P., Dean, W. L., and Whiteheart, S. W. (2003) A role for Sec1/Munc18 proteins in platelet exocytosis. *Biochem. J.* **374,** 207–217 CrossRef Medline
32. Oh, E., Spurlin, B. A., Pessin, J. E., and Thurmond, D. C. (2005) Munc18c heterozygous knockout mice display increased susceptibility for severe glucose intolerance. *Diabetes* **54,** 638–647 CrossRef Medline
33. Kanda, H., Tamori, Y., Shinoda, H., Yoshikawa, M., Sakaue, M., Udagawa, J., Otani, H., Tashiro, F., Miyazaki, J., and Kasuga, M. (2005) Adipocytes from Munc18c-null mice show increased sensitivity to insulin-stimulated GLUT4 externalization. *J. Clin. Invest.* **115,** 291–301 CrossRef Medline
34. Jewell, J. L., Oh, E., and Thurmond, D. C. (2010) Exocytosis mechanisms underlying insulin release and glucose uptake: conserved roles for Munc18c and syntaxin 4. *Am. J. Physiol. Regul. Integr. Comp. Physiol.* **298,** R517–R531 CrossRef Medline
35. Tamori, Y., Kawanishi, M., Niki, T., Shinoda, H., Araki, S., Okazawa, H., and Kasuga, M. (1998) Inhibition of insulin-induced GLUT4 translocation by Munc18c through interaction with syntaxin4 in 3T3-L1 adipocytes. *J. Biol. Chem.* **273,** 19740–19746 CrossRef Medline
36. Tellam, J. T., Macaulay, S. L., McIntosh, S., Hewish, D. R., Ward, C. W., and James, D. E. (1997) Characterization of Munc-18c and syntaxin-4 in 3T3-L1 adipocytes. Putative role in insulin-dependent movement of GLUT-4. *J. Biol. Chem.* **272,** 6179–6186 CrossRef Medline
37. Hu, S. H., Latham, C. F., Gee, C. L., James, D. E., and Martin, J. L. (2007) Structure of the Munc18c/Syntaxin4 N-peptide complex defines universal features of the N-peptide binding mode of Sec1/Munc18 proteins. *Proc. Natl. Acad. Sci. U.S.A.* **104,** 8773–8778 CrossRef Medline
38. Paumet, F., Le Mao, J., Martin, S., Galli, T., David, B., Blank, U., and Roa, M. (2000) Soluble NSF attachment protein receptors (SNAREs) in RBL-2H3 mast cells: functional role of syntaxin 4 in exocytosis and identification of a vesicle-associated membrane protein 8-containing secretory compartment. *J. Immunol.* **164,** 5850–5857 CrossRef Medline
39. Sander, L. E., Frank, S. P., Bolat, S., Blank, U., Galli, T., Bigalke, H., Bischoff, S. C., and Lorentz, A. (2008) Vesicle associated membrane protein (VAMP)-7 and VAMP-8, but not VAMP-2 or VAMP-3, are required for activation-induced degranulation of mature human mast cells. *Eur. J. Immunol.* **38,** 855–863 CrossRef Medline
40. Salinas, E., Quintanar-Stephano, A., Córdova, L. E., and Ouintanar, J. L. (2008) Allergen-sensitization increases mast-cell expression of the exocytotic proteins SNAP-23 and syntaxin 4, which are involved in histamine secretion. *J. Investig. Allergol. Clin. Immunol.* **18,** 366–371 Medline
41. Woska, J. R., Jr., and Gillespie, M. E. (2011) Small-interfering RNA-mediated identification and regulation of the ternary SNARE complex mediating RBL-2H3 mast cell degranulation. *Scand. J. Immunol.* **73,** 8–17 CrossRef Medline
42. Blank, U., Cyprien, B., Martin-Verdeaux, S., Paumet, F., Pombo, I., Rivera, J., Roa, M., and Varin-Blank, N. (2002) SNAREs and associated regulators in the control of exocytosis in the RBL-2H3 mast cell line. *Mol. Immunol.* **38,** 1341–1345 CrossRef Medline
43. Woska, J. R., Jr., and Gillespie, M. E. (2012) SNARE complex-mediated degranulation in mast cells. *J. Cell. Mol. Med.* **16,** 649–656 CrossRef Medline
44. Baram, D., Adachi, R., Medalia, O., Tuvim, M., Dickey, B. F., Mekori, Y. A., and Sagi-Eisenberg, R. (1999) Synaptotagmin II negatively regulates Ca^{2+}-triggered exocytosis of lysosomes in mast cells. *J. Exp. Med.* **189,** 1649–1658 CrossRef Medline
45. Scholten, J., Hartmann, K., Gerbaulet, A., Krieg, T., Müller, W., Testa, G., and Roers, A. (2008) Mast cell-specific Cre/loxP-mediated recombination *in vivo*. *Transgenic Res.* **17,** 307–315 CrossRef Medline
46. Verhage, M., Maia, A. S., Plomp, J. J., Brussaard, A. B., Heeroma, J. H., Vermeer, H., Toonen, R. F., Hammer, R. E., van den Berg, T. K., Missler, M., Geuze, H. J., and Südhof, T. C. (2000) Synaptic assembly of the brain in the absence of neurotransmitter secretion. *Science* **287,** 864–869 CrossRef Medline
47. Alvarez de Toledo, G., and Fernandez, J. M. (1990) Patch-clamp measurements reveal multimodal distribution of granule sizes in rat mast cells. *J. Cell Biol.* **110,** 1033–1039 CrossRef Medline
48. Fernandez, J. M., Neher, E., and Gomperts, B. D. (1984) Capacitance measurements reveal stepwise fusion events in degranulating mast cells. *Nature* **312,** 453–455 CrossRef Medline
49. Neher, E. (1988) The influence of intracellular calcium concentration on degranulation of dialysed mast cells from rat peritoneum. *J. Physiol.* **395,** 193–214 CrossRef Medline
50. Tatham, P. E., and Gomperts, B. D. (1991) Rat mast cells degranulate in response to microinjection of guanine nucleotide. *J. Cell Sci.* **98,** 217–224 Medline
51. Oberhauser, A. F., and Fernandez, J. M. (1996) A fusion pore phenotype in mast cells of the ruby-eye mouse. *Proc. Natl. Acad. Sci. U.S.A.* **93,** 14349–14354 CrossRef Medline
52. Finkelstein, A., Zimmerberg, J., and Cohen, F. S. (1986) Osmotic swelling of vesicles: its role in the fusion of vesicles with planar phospholipid bilayer membranes and its possible role in exocytosis. *Annu. Rev. Physiol.* **48,** 163–174 CrossRef Medline
53. Ozawa, K., Szallasi, Z., Kazanietz, M. G., Blumberg, P. M., Mischak, H., Mushinski, J. F., and Beaven, M. A. (1993) Ca^{2+}-dependent and Ca^{2+}-independent isozymes of protein kinase C mediate exocytosis in antigen-stimulated rat basophilic RBL-2H3 cells: reconstitution of secretory responses with Ca^{2+} and purified isozymes in washed permeabilized cells. *J. Biol. Chem.* **268,** 1749–1756 Medline
54. Schwartz, L. B., Lewis, R. A., Seldin, D., and Austen, K. F. (1981) Acid hydrolases and tryptase from secretory granules of dispersed human lung mast cells. *J. Immunol.* **126,** 1290–1294 Medline
55. Lieberman, P., and Garvey, L. H. (2016) Mast cells and anaphylaxis. *Curr. Allergy Asthma Rep.* **16,** 20 CrossRef Medline
56. Makabe-Kobayashi, Y., Hori, Y., Adachi, T., Ishigaki-Suzuki, S., Kikuchi, Y., Kagaya, Y., Shirato, K., Nagy, A., Ujike, A., Takai, T., Watanabe, T., and Ohtsu, H. (2002) The control effect of histamine on body temperature and respiratory function in IgE-dependent systemic anaphylaxis. *J. Allergy Clin. Immunol.* **110,** 298–303 CrossRef Medline
57. Bugajski, J., and Zacny, E. (1981) The role of central histamine H1- and H2-receptors in hypothermia induced by histamine in the rat. *Agents Actions* **11,** 442–447 CrossRef Medline
58. Latham, C. F., Lopez, J. A., Hu, S. H., Gee, C. L., Westbury, E., Blair, D. H., Armishaw, C. J., Alewood, P. F., Bryant, N. J., James, D. E., and Martin, J. L. (2006) Molecular dissection of the Munc18c/syntaxin4 interaction: implications for regulation of membrane trafficking. *Traffic* **7,** 1408–1419 CrossRef Medline
59. Thurmond, D. C., Ceresa, B. P., Okada, S., Elmendorf, J. S., Coker, K., and Pessin, J. E. (1998) Regulation of insulin-stimulated GLUT4 translocation

by Munc18c in 3T3L1 adipocytes. *J. Biol. Chem.* **273,** 33876–33883 CrossRef Medline

60. Imai, A., Nashida, T., and Shimomura, H. (2004) Roles of Munc18-3 in amylase release from rat parotid acinar cells. *Arch. Biochem. Biophys.* **422,** 175–182 CrossRefMedline
61. Araki, S., Tamori, Y., Kawanishi, M., Shinoda, H., Masugi, J., Mori, H., Niki, T., Okazawa, H., Kubota, T., and Kasuga, M. (1997) Inhibition of the binding of SNAP-23 to syntaxin 4 by Munc18c. *Biochem. Biophys. Res. Commun.* **234,** 257–262 CrossRef Medline
62. ter Beest, M. B., Chapin, S. J., Avrahami, D., and Mostov, K. E. (2005) The role of syntaxins in the specificity of vesicle targeting in polarized epithelial cells. *Mol. Biol. Cell* **16,** 5784–5792 CrossRef Medline
63. Fu, J., Naren, A. P., Gao, X., Ahmmed, G. U., and Malik, A. B. (2005) Protease-activated receptor-1 activation of endothelial cells induces protein kinase Cα-dependent phosphorylation of syntaxin 4 and Munc18c: role in signaling p-selectin expression. *J. Biol. Chem.* **280,** 3178–3184 CrossRef Medline
64. Puri, N., and Roche, P. A. (2006) Ternary SNARE complexes are enriched in lipid rafts during mast cell exocytosis. *Traffic* **7,** 1482–1494 CrossRef Medline
65. Brochetta, C., Suzuki, R., Vita, F., Soranzo, M. R., Claver, J., Madjene, L. C., Attout, T., Vitte, J., Varin-Blank, N., Zabucchi, G., Rivera, J., and Blank, U. (2014) Munc18-2 and syntaxin 3 control distinct essential steps in mast cell degranulation. *J. Immunol.* **192,** 41–51CrossRef Medline
66. Hata, Y., and Südhof, T. C. (1995) A novel ubiquitous form of Munc-18 interacts with multiple syntaxins. Use of the yeast two-hybrid system to study interactions between proteins involved in membrane traffic. *J. Biol. Chem.* **270,** 13022–13028 CrossRef Medline
67. Dulubova, I., Yamaguchi, T., Arac, D., Li, H., Huryeva, I., Min, S. W., Rizo, J., and Sudhof, T. C. (2003) Convergence and divergence in the mechanism of SNARE binding by Sec1/Munc18-like proteins. *Proc. Natl. Acad. Sci. U.S.A.* **100,** 32–37 CrossRef Medline
68. Christie, M. P., Hu, S. H., Whitten, A. E., Rehman, A., Jarrott, R. J., King, G. J., Collins, B. M., and Martin, J. L. (2017) Revisiting interaction specificity reveals neuronal and adipocyte Munc18 membrane fusion regulatory proteins differ in their binding interactions with partner SNARE Syntaxins. *PLoS One* **12,** e0187302 CrossRef Medline
69. Dernick, G., de Toledo, G. A., and Lindau, M. (2007) The patch amperometry technique: design of a method to study exocytosis of single vesicles. In *Electrochemical Methods for Neuroscience* (Michael, A. C., and Borland, L. M., eds) pp. 315–336, CRC Press/Taylor & Francis, Boca Raton, FL
70. Grimbaldeston, M. A., Chen, C. C., Piliponsky, A. M., Tsai, M., Tam, S. Y., and Galli, S. J. (2005) Mast cell-deficient W-sash c-kit mutant Kit W-sh/W-sh mice as a model for investigating mast cell biology *in vivo*. *Am. J. Pathol.* **167,** 835–848 CrossRef Medline
71. Stevens, R. L., Friend, D. S., McNeil, H. P., Schiller, V., Ghildyal, N., and Austen, K. F. (1994) Strain-specific and tissue-specific expression of mouse mast cell secretory granule proteases. *Proc. Natl. Acad. Sci. U.S.A.* **91,** 128–132 CrossRef Medline
72. Gurish, M. F., and Austen, K. F. (2012) Developmental origin and functional specialization of mast cell subsets. *Immunity* **37,** 25–33 CrossRef Medline
73. Ginsburg, H., Ben-Shahar, D., and Ben-David, E. (1982) Mast cell growth on fibroblast monolayers: two-cell entities. *Immunology* **45,** 371–380 Medline
74. Irani, A. M., Craig, S. S., DeBlois, G., Elson, C. O., Schechter, N. M., and Schwartz, L. B. (1987) Deficiency of the tryptase-positive, chymase-negative mast cell type in gastrointestinal mucosa of patients with defective T lymphocyte function. *J. Immunol.* **138,** 4381–4386 Medline
75. Ruitenberg, E. J., and Elgersma, A. (1976) Absence of intestinal mast cell response in congenitally athymic mice during *Trichinella spiralis* infection. *Nature* **264,** 258–260 CrossRef Medline
76. McNeil, H. P., Frenkel, D. P., Austen, K. F., Friend, D. S., and Stevens, R. L. (1992) Translation and granule localization of mouse mast cell protease-5: immunodetection with specific antipeptide Ig. *J. Immunol.* **149,** 2466–2472 Medline
77. Friend, D. S., Ghildyal, N., Austen, K. F., Gurish, M. F., Matsumoto, R., and Stevens, R. L. (1996) Mast cells that reside at different locations in the jejunum of mice infected with *Trichinella spiralis* exhibit sequential changes in their granule ultrastructure and chymase phenotype. *J. Cell Biol.* **135,** 279–290 CrossRef Medline
78. Heeroma, J. H., Roelandse, M., Wierda, K., van Aerde, K. I., Toonen, R. F., Hensbroek, R. A., Brussaard, A., Matus, A., and Verhage, M. (2004) Trophic support delays but does not prevent cell-intrinsic degeneration of neurons deficient for munc18–1. *Eur. J. Neurosci.* **20,** 623–634 CrossRef Medline
79. Adachi, R., Krilis, S. A., Nigrovic, P. A., Hamilton, M. J., Chung, K., Thakurdas, S. M., Boyce, J. A., Anderson, P., and Stevens, R. L. (2012) Ras guanine nucleotide-releasing protein-4 (RasGRP4) involvement in experimental arthritis and colitis. *J. Biol. Chem.* **287,** 20047–20055 CrossRef Medline
80. Tschanz, S. A., Burri, P. H., and Weibel, E. R. (2011) A simple tool for stereological assessment of digital images: the STEPanizer. *J. Microsc.* **243,** 47–59 CrossRef Medline
81. Brock, T. A., Dennis, P. A., Griendling, K. K., Diehl, T. S., and Davies, P. F. (1988) GTP gamma S loading of endothelial cells stimulates phospholipase C and uncouples ATP receptors. *Am. J. Physiol.* **255,** C667–C673 CrossRef Medline
82. Messler, P., Harz, H., and Uhl, R. (1996) Instrumentation for multiwavelengths excitation imaging. *J. Neurosci. Methods* **69,** 137–147 CrossRef Medline
83. Grynkiewicz, G., Poenie, M., and Tsien, R. Y. (1985) A new generation of Ca^{2+} indicators with greatly improved fluorescence properties. *J. Biol. Chem.* **260,** 3440–3450 Medline
84. Innocenti, B., and Heidelberger, R. (2008) Mechanisms contributing to tonic release at the cone photoreceptor ribbon synapse. *J. Neurophysiol.* **99,** 25–36 CrossRef Medline
85. Lindau, M., and Neher, E. (1988) Patch-clamp techniques for time-resolved capacitance measurements in single cells. *Pflugers Arch.* **411,** 137–146 CrossRef Medline
86. Gillis, K. D. (1995) Techniques for membrane capacitance measurements. In *Single-Channel Recording* (Sakmann, B., and Neher, E., eds) pp. 155–198, Springer, Boston, MA